Vibrations of Fractal Drums

B. Sapoval, Th. Gobron, and A. Margolina[(a)]
Laboratoire de Physique de la Matière Condensée, Ecole Polytechnique, 91128 Palaiseau CEDEX, France
(Received 17 July 1991)

Fractal boundary conditions drastically alter wave excitations. The low-frequency vibrations of a membrane bounded by a rigid fractal contour are observed and localized modes are found. The first lower eigenmodes are computed using an analogy between the wave and the diffusion equations. The fractal frontier induces a strong confinement of the wave analogous to superlocalization. The wave forms exhibit singular derivatives near the boundary.

PACS numbers: 64.60.Ak, 03.40.Kf, 63.50.+x, 71.55.Jv

Objects with irregular geometry are ubiquitous in nature and their vibrational properties are of general interest. For instance, the dependence of sea waves on the topography of coastlines is a largely unanswered question. The emergence of fractal geometry was a significant breakthrough in the description of irregularity [1]. It has been suggested that the very existence of some of the fractal structures found in nature is attributable to a self-stabilization due to their ability to damp harmonic excitations [2]. In this hypothesis, fractal coastlines are best at damping waves and are submitted to weaker erosion. Fractals having no translational invariance cannot transmit ordinary waves. Mass fractal vibrations, called fractons, are generally localized [3]. The problem which we address is the vibration of a surface fractal (the fractal bounded resonator) [4]. We present the first results of an experimental and theoretical investigation of the properties of a 2D fractal drum.

The main properties of resonators are the structure of the vibration modes, their spectrum, and their damping. Up to now, only the asymptotic density of states of fractal drums has been discussed from a mathematical point of view [5]. The drum used in the experiment has the pattern shown in Fig. 1(b). This contour has been machined by laser etching in a stainless-steel sheet (ca. 0.5 mm). The membrane is either a "soap bubble" or a stretched plastic film. The setup is sketched in Fig. 1(c). The vibrations, from 15 Hz and above, are generated by a loudspeaker placed 10 cm above the drum. Soap bubbles are somewhat difficult to photograph and are unstable. To photograph the wave form we used a membrane made of streched plastic film (ca. 5 μm) on which a fine powder has been sprinkled. We tested that the tension of the membrane was uniform by examining it under cross polarizers. The powder was agitated by the vertical motion of the membrane. This allowed for direct observation of the vibrating regions of the membrane.

The lowest frequency mode shows no node line as predicted by general mathematical results [6]. The vibration has a maximum at the center of the drum and decays rapidly when entering the side regions. At higher frequencies more complex resonances are observed. The most striking fact is the observation of vibrations which are confined in a finite region of the membrane like region A in Fig. 1(b). A photograph of a localized mode is shown in Fig. 2.

The observation of confined modes was a surprise because, in principle, the symmetry of the structure forbids their existence. In fact, this experimental localization is due both to damping and to the existence of narrow paths in the geometry of the membrane. If only one of the equivalent regions like A is excited, then a certain time T_l called the delocalization time is necessary for the excitation to travel from A to B. For a narrow pipe this time is very long. But a real oscillator always has finite losses which create damping. A given resonance decays in a time $T_d = Q\omega^{-1}$, where Q is the quality factor of the res-

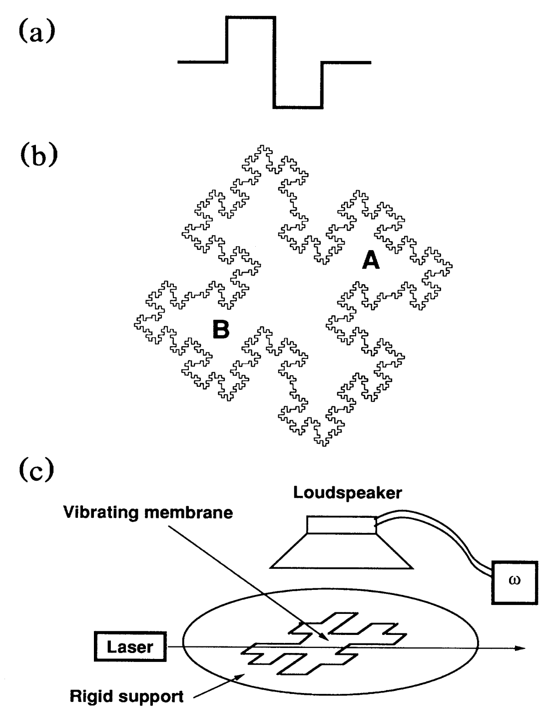

FIG. 1. Fractal drum and experimental setup. (a) The fractal generator. (b) Drum perimeter after three iterations from a square initiator. Fractal dimension $D=\frac{3}{2}$. (c) Diagram of the experiment: The variable frequency generator feeds a loudspeaker which excites, through the air, the membrane acoustic vibrations. These vibrations can be detected by the change in the He-Ne laser reflection.

FIG. 2. Still photograph of a localized vibration (exposure time 1 s). In the vibrating region the light of the grazing laser is strongly scattered.

onance. The possibility of observing a localized mode then depends on T_l and T_d. If the damping is weak ($T_l < T_d$), the excitation can propagate from A to B. If $T_l > T_d$, the excitation will be damped before reaching B and localized modes can be observed. The coupling of two regions connected by a narrow path is shown schematically in Fig. 3(a). A wave of wavelength Λ propagates in a path narrower than $\Lambda/2$ with exponential attenuation $\psi \sim (a/\Lambda)\exp(-x\pi/a)$ [7]. If the drums of Fig. 3(a) were isolated, the two modes ψ_A and ψ_B would have the same frequency. If the two drums were communicating, the eigenmodes would now be the combinations $\psi_A + \psi_B$ and $\psi_A - \psi_B$ and there would exist a frequency splitting $\delta\omega$ between the two modes. The effective coupling between the two drums at distance Δ is, in reduced units, of order $(a/\Lambda)^2\exp(-\pi\Delta/a)$. The splitting between the new modes is given approximately by $\delta\omega \approx (\omega/2)(a/\Lambda)^2\exp(-\pi\Delta/a)$. The inverse of the splitting $\delta\omega$ is the delocalization time T_l.

In our experiment the geometry is more similar to Fig. 3(b) in which A and B are coupled through a narrow path but across a wider resonator. To evaluate the coupling in this situation we use ordinary Rayleigh perturbation theory [6]. With no coupling the four lower states are $\psi_{0,s}, \psi_{0,as}$, lower symmetric and antisymmetric states of the central resonator, and ψ_A, ψ_B, with the energies $E_{0,s}$, $E_{0,as}$, E_A, and $E_B = E_A$. We chose to work in the equivalent basis $\psi_{0,s}$, $\psi_{0,as}$, $\psi_A + \psi_B$, and $\psi_A - \psi_B$ in which the unperturbed Hamiltonian is diagonal. If the resonators communicate, there will exist a coupling but only between states of same symmetry, i.e., $\psi_{0,s};(\psi_A + \psi_B)$ and $\psi_{0,as};(\psi_A - \psi_B)$. It is then only at the second order in perturbation that the degeneracy can be removed. The effective coupling between $(\psi_A + \psi_B)$ and $(\psi_A - \psi_B)$ is, in reduced units, of order $[(a/\Lambda)^2 \times\exp(-\pi\Delta/a)]^2$. This coupling is very small resulting in very large values for T_l. Note that this effect is due to the existence of narrow paths which are not necessarily present in all fractal drums.

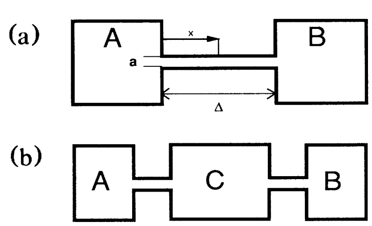

FIG. 3. Localization by damping. Top: drums coupled by a narrow path. Bottom: succession of narrow and larger paths. If the frequencies of the central states are not resonant with A or B frequencies, there exists only a very weak second-order coupling.

To better account for the observed effects, we have computed numerically the lowest modes. We use the analogy between the Helmholtz equation, $\Delta z - (1/c^2)\partial^2 z/\partial t^2 = 0$, where c is the wave velocity, and the diffusion equation, $\Delta z - (1/D)\partial z/\partial t = 0$, where D is the diffusion coefficient, with the boundary condition, $z = 0$, on the contour. The general solution of the diffusion equation is

$$z(x,y,t) = \sum_n \Psi_n(x,y)\exp(-\lambda_n t)\,, \tag{1}$$

with $\Psi_n(x,y)$ a solution of the eigenvalue equation $\Delta\Psi = (-\lambda/D)\Psi$ or identically $\Delta\Psi = (-\omega^2/c^2)\Psi$ provided that

$$\lambda/D = \omega^2/c^2\,. \tag{2}$$

The set of solutions (Ψ_n,λ_n) is ordered by increasing values of λ_n with $\lambda_0 \le \lambda_1 \le \lambda_2 \le \cdots \lambda_n \le \cdots$ and the modes are computed sequentially. We start from an arbitrary function $z_0(x,y,t=0)=L^{-1}$ as an initial distribution and compute numerically its evolution using the diffusion equation. (We used a constant $z=L^{-1}$ where L is the side of the square fractal initiator.) After a given time, due to the hierarchy of the λ_n's we are left with the wave form of the fundamental decaying with a single time constant λ_0 and the fundamental frequency is found from Eq. (2). We start again with a new initial function z_1 that we chose to be orthogonal to $\Psi_0(x,y)$, and repeat the procedure [6]. The diffusion equation has been discretized both in space and in time. The computation took place on a square grid (2^{16} inner points) compatible with the boundary. In the case of the square drum, exact solutions are known analytically for both continuous and discretized equations [8] and from that we estimate the error due to space discretization to be less than 10^{-3}. Time discretization leads to the replacement of $\exp(-t/\tau)$ by a power law $[\exp(-\Delta t/\tau)]^{t/\Delta t}$, and therefore can be corrected. Numerical errors are determined by the difference which we permit between the computed modes decay and a single exponential decay. We have chosen this deviation such that the relative accuracy on the eigenvalue is better than 10^{-5} as verified for the square drum. The first five lower modes of the fractal pattern were computed. The fundamental state is shown in Fig. 4(a). It is centered in the central part of the drum and corresponds to $\Omega=2.100\omega_0$, where $\omega_0=2^{1/2}\pi c/L$ is the fundamental frequency of the initiator. The figure shows that the amplitude decays strongly from the center towards the edges of the drum. This is shown in Fig. 4(b) where the logarithm of the amplitude is represented. The fact that the slope of the "mountain" increases when reaching the deepest bay is a confinement effect reminiscent of a superlocalization behavior [9] and will be discussed in more detail elsewhere [10]. Note that the irregularity of the frontier of the drum markedly shifts the fundamental mode to a higher frequency.

The next four modes with frequencies of $\Omega_1=\Omega_2=3.132\omega_0$, $\Omega_3=3.191\omega_0$, and $\Omega_4=3.219\omega_0$ are shown in Fig. 5. From these values the delocalization time T_l is of order $\sim 40\omega_0^{-1}$. From the width of the experimental response a quality factor of order 10 was measured. This gives $T_d \sim 10\omega_0^{-1} < T_l$, which is the condition for localization by damping. None of these modes are localized but a localized linear superposition of these modes is shown at the bottom of Fig. 5. It compares favorably with the photograph of Fig. 2. The experimental value of the frequency of this mode is found to be equal to $1.7\Omega_0$ instead of $1.54\Omega_0$, as predicted using the above numbers. The discrepancy can probably be attributed to a small admixture of a higher excited state [10]. The computed wave forms also confirm the existence of singularities very near the wedges: The derivatives of the wave form

(a)

(b)

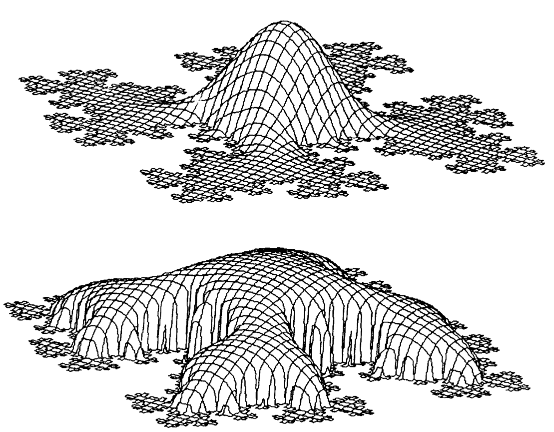

FIG. 4. Top: Wave form of the fundamental vibration. Bottom: logarithm of the wave form showing a faster than exponential decay of the amplitude towards the edges of the drum. The value of the logarithm has been truncated below a finite value.

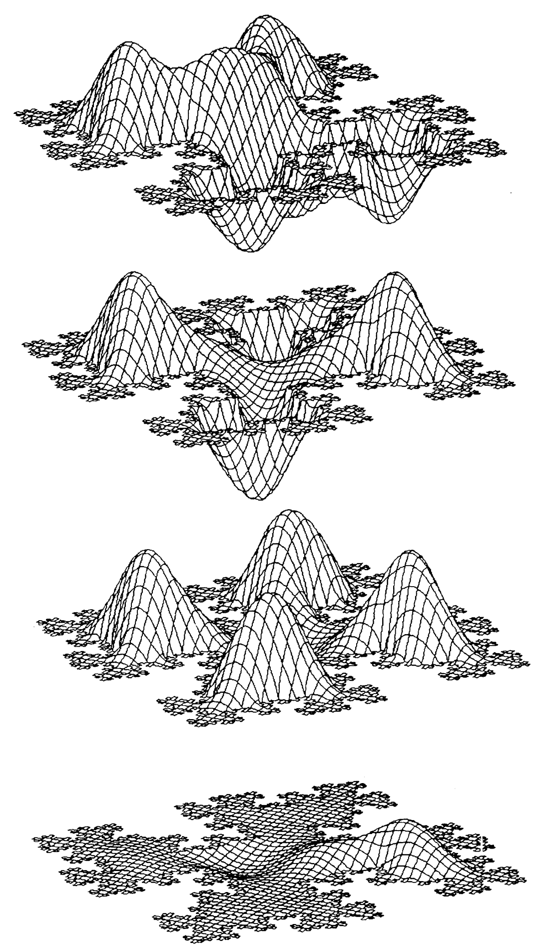

FIG. 5. Second to fifth excited states. From top to bottom, state 2 or 3 (degenerate through a rotation of $\pi/2$), state 4, state 5, and a localized linear combination of the second to the fifth excited states. This image is to be compared with Fig. 2.

are infinite at salient points [11].

In conclusion, we have shown both experimentally and numerically that fractal boundaries may alter drastically the spatial character of waves. The geometry imposes a very strong spatial decay of the wave form inside fractal cavities. The modes are shifted to higher frequencies and the wave form shows singularities on the frontier.

A few tentative comments can be made because of these results. These effects should appear in the vibrations of rough microcrystalline atomic arrangements, as the internal interfaces in mixed glasses [12] may naturally possess the fractal geometry of diffusion fronts [13]. The quantum states in small-scale irregular structures like porous silicon, a material of possible fractal geometry [14], should also show the same characteristics.

Current knowledge about waves and resonators indicates that small changes in the boundary geometry of resonators can modify strongly the damping properties. High-quality-factor wave guides and microwave cavities are polished. Irregularities in the geometry of the boundary cause singularities in the electric field which can lead to dielectric breakdown. Coastline engineers use porous structures empirically made of disordered heaps of rocks of various sizes, to absorb energy when designing breakwaters [15]. The geometry of anechoic chambers is another possible illustration. In physical systems bounded by fractals, nonlinear effects should be present due to the existence of singularities on the wedges. For all these reasons, fractal structures should be efficient in damping vibrations and waves. This can be the key to a "self-stabilization" of many of the fractal structures found in nature.

Laboratoire de Physique de la Matière Condensée is Unité associée du CNRS No. 1254.

(a)Permanent address: Physics Department, Polytechnic University, 333 Jay Street, Brooklyn, NY 11201.

[1] B. B. Mandelbrot, *The Fractal Geometry of Nature* (Freeman, San Francisco, 1982).

[2] B. Sapoval, *Fractals* (Aditech, Paris, 1990).

[3] S. Alexander and R. Orbach, J. Phys. (Paris), Lett. **43**, L625 (1982); R. Rammal and G. Toulouse, J. Phys. (Paris), Lett. **44**, L13 (1983).

[4] M. V. Berry, *Structural Stability in Physics*, edited by W. Guttinger and H. Elkeimer (Springer-Verlag, Berlin, 1979), pp. 51–53.

[5] M. L. Lapidus, Trans. Am. Math. Soc. **325**, 2 (1991); **325**, 465 (1991), and references therein.

[6] R. Courant and D. Hilbert, *Methods of Mathematical Physics* (Interscience, New York, 1965).

[7] See, for instance, C. D. Jackson, *Classical Electrodynamics* (Wiley, New York, 1975), p. 344.

[8] C. Kittel, *Introduction to Solid State Physics* (Wiley, New York, 1976).

[9] A. Aharony and A. Brooks Harris, Physica (Amsterdam) **163A**, 38 (1990).

[10] B. Sapoval and Th. Gobron (to be published).

[11] B. Sapoval, Physica (Amsterdam) **38D**, 296 (1989).

[12] A. Fontana, F. Rocca, M. P. Fontana, B. Rosi, and A. J. Dianoux, Phys. Rev. B **41**, 3778 (1990).

[13] B. Sapoval, M. Rosso, and J.-F. Gouyet, in *The Fractal Approach to Heterogeneous Chemistry*, edited by D. Avnir (Wiley, New York, 1989), p. 227.

[14] P. Goudeau, A. Naudon, G. Bomchil, and R. Herino, J. Appl. Phys. **66**, 2 (1989); **66**, 625 (1989).

[15] B. Le Méhauté, in *The Encyclopedia of Applied Geology*, edited by Ch. W. Finkl, Jr. (Van Nostrand and Reinhold, New York, 1984), p. 62.

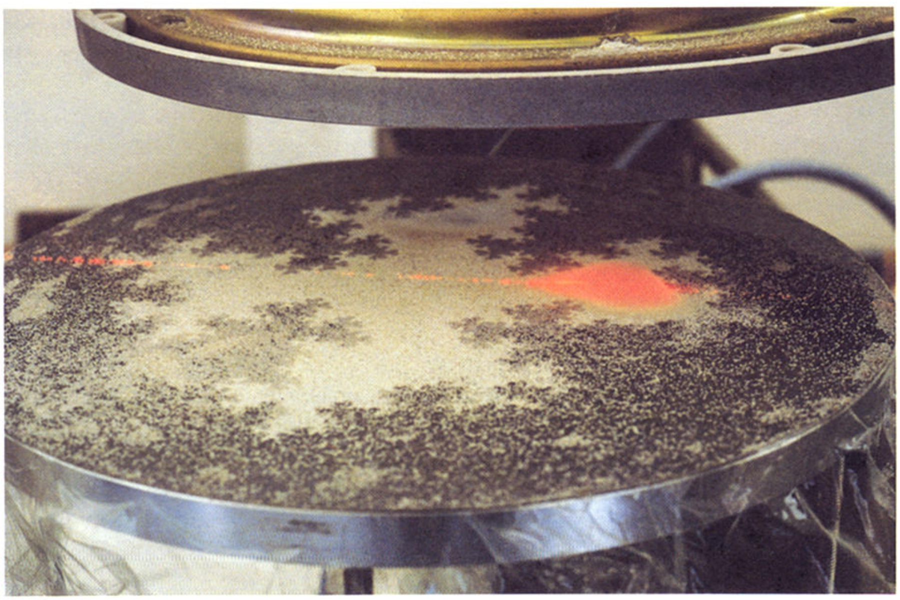

FIG. 2. Still photograph of a localized vibration (exposure time 1 s). In the vibrating region the light of the grazing laser is strongly scattered.